Phase Equilibrium in the System Ln-Mn-O at 1100℃

Ⅸ. Ln = Er and Tm

Kenzo KITAYAMA*, Natsuko SHIOYA**, Motohiro IURA***, Syunsuke IKEDA***, Naoki SAEKI****, and Yuzuru ISHIZAWA*****

(Received October 31, 2007)

Phase equilibrium was established in a Ln-Mn-O (Ln = Er and Tm) system at 1100 ℃ with the oxygen partial pressure ranging from $-\log (P_{O_2}/atm) = 0$ to 12.00, and phase diagrams for the corresponding Ln_2O_3-MnO-MnO_2 system at 1100℃ were constructed. Stable Er_2O_3, MnO, Mn_3O_4, and $ErMnO_3$ phases were found in the Er-Mn-O system, and stable Tm_2O_3, MnO, Mn_3O_4, and $TmMnO_3$ phases were found in the Tm-Mn-O system.

$LnMn_2O_5$, $Ln_2Mn_2O_7$, Ln_2MnO_4, Mn_2O_3, and MnO_2 were not found in either system.

Nonstoichiometric ranges were found in both $LnMnO_3$ phases, with the composition of $LnMnO_3$ represented as functions of log (P_{O_2}/atm), $No/N_{ErMnO_3} = 2.68\times10^{-3} (\log P_{O_2}) - 0.008$ and $No/N_{TmMnO_3} = 2.53 \times10^{-3} \log (P_{O_2}) - 0.005$

The activities of the components in a solid solution were calculated from the both equations.

The lattice constants of $ErMnO_3$ and $TmMnO_3$ quenched in air were determined.

The standard Gibbs energy changes of the reaction, $1/2\ Ln_2O_3 + MnO + 1/4\ O_2 = LnMnO_3$, appearing in the phase diagrams were also calculated. The relationship between the tolerance factors (t) of $ErMnO_3$, $TmMnO_3$ and ΔG^0 values of the reaction, $1/2\ Ln_2O_3 + MnO + 1/4\ O_2 = LnMnO_3$, was shown graphically, together with other previous $LnMnO_3$ values. The two present ΔG^0 values were well-fitted to the general equation for hexagonal $LnMnO_3$, ΔG^0 (hexa) $= -6.426\times10^2\ t + 5.406\times10^2$, which was previously obtained.

Key words: Phase equilibrium; Thermogravimetry; Erbium-manganese oxide; Thulium manganese oxide; Gibbs energy.

1. INTRODUCTION

A number of reports have dealt with the magnetic, electronic, and crystallographic properties of $LaMnO_3$ (1,2). The magnetic order, moments, and ordering tempera-

* Emeritus Professor of Niigata Institute of Technology

** A graduate, 2002

*** A graduate, 2004

**** A graduate, 2005

***** A graduate, 2006

tures of $La_{1-t}MnO_{3+\delta}$ depend strongly on the non-stoichiometry (3), and a series on the defect chemistry of $LaMnO_{3\pm\delta}$ was reported by Van Roosmalen et al.(4). Although similar physical properties would be expected in other perovskit-structured lanthanoid-manganese-oxides, only a few phase diagram studies that could precisely reveal the non-stoichiometry of $LnMnO_3$ have been performed (5,6).

Recently, the phase equilibrium has been established in Ln-Mn-O systems at 1100℃ (Ln = La (7), Nd (8), Gd (9), Sm (10), Yb and Dy (11), Ho and Tb (12), Eu and Y (13), and Pr and Lu (14)). According to these studies, there are two types of phase diagrams depending on the number of stable ternary compounds in the Ln-Mn-O system, one being the single ternary compound $LnMnO_3$ and the other two ternary compounds, $LnMnO_3$ and $LnMn_2O_5$. But on account of the stability of Pr_6O_{11} under the present experimental conditions in the Pr-O system, the pattern of the Pr-Mn-O system (14) is different from the latter type with two ternary compounds.

The objectives of the present study are to: (1) establish detailed phase diagrams of the Er-Mn-O and Tm-Mn-O systems at 1100℃ as a function of the oxygen partial pressure, (2) know to which types of the phase diagram these established systems belong, (3) determine the thermochemical properties based on the phase equilibrium at 1100℃, and (4) plot ΔG^0 values of the common reaction, $1/2\ Ln_2O_3 + MnO + 1/4\ O_2 = LnMnO_3$, for both systems on the previous line of ΔG^0 vs. tolerance factor.

2. EXPERIMENTAL

Analytical grade Er_2O_3 (99.9%), Tm_2O_3 (99.9%), and MnO (99.9%) were used as starting- materials.

The MnO was dried by heating it in air at 110℃, and both of the other oxides were calcined at 1100℃. Mixtures with the desired ratio of Ln_2O_3 to MnO were prepared by mixing thoroughly in an agate mortar and performing repeated calcination during the intermediate mixing. This was followed by the same procedures described previously (15). The thermogravimetric method was used in the present experiment; the oxygen partial pressure was adjusted by passing a gas or mixed gases through the furnace.

The desired oxygen partial pressures were obtained using gas mixtures of CO_2 and H_2 and of CO_2 and O_2, and the single-component gases O_2 and CO_2. The apparatus and procedures for controlling the oxygen partial pressure and maintaining a constant temperature, the method of thermogravimetry, and the criterion for the establishment

of equilibrium were the same as described in the previous paper (15). The method for establishing equilibrium can be described briefly as follows. To ensure equilibrium, the equilibrium weight of each sample at a particular oxygen partial pressure was determined from both sides of the reaction; that is, as the oxygen partial pressure was increasing from a lower value and as it was decreasing from a higher value. The balance, furnace, and gas mixer are schematically shown in (16). The furnace was installed vertically, and a mullite tube wound with Pt 60%-Rh 40% alloy wire served as its heating element. Mixed gases, which ensure the desired oxygen partial pressures, passed from the bottom of the furnace to the top. The actual oxygen partial pressures of the gas phase were measured by means of a solid electrolytic cell composed of $(ZrO_2)_{0.85}(CaO)_{0.15}$ (17).

The identification of phases and the determination of lattice constants were performed using a Rint 2500 Rigaku X-ray diffractometer, with Ni-filtered CuK α radiation. An external standard silicon was used to calibrate 2θ.

3. RESULTS AND DISCUSSIONS

3-1. Phase equilibrium

3-1-1. Mn-O system

Four oxides, MnO, Mn_3O_4, Mn_2O_3, and MnO_2, have been noted in the Mn-O system. This system was reinvestigated under the present experimental conditions and has been reported in the La_2O_3-MnO-MnO_2 system (7). The oxygen partial pressure in equilibrium with MnO and Mn_3O_4 was found to be log (P_{O_2}/atm) = -5.40 ± 0.05 and Mn_3O_4 was stoichiometric over the range of $-\log$ (P_{O_2}/atm) = 0 to 5.40. MnO, however, is slightly nonstoichiometric, being oxygen-rich with a O/Mn molar ratio of 1.019 at log (P_{O_2}/atm) = -5.40. An equation, $N_O/N_{MnO} = 9.83\times10^{-4}(\log P_{O_2})^2 + 1.914\times10^{-2}(\log P_{O_2}) + 0.0933$, was obtained for the MnO solid solution over the oxygen partial pressure range from -10.00 to -5.40 using the least squares method. Here, we supposed that the MnO solid solution consisted of two components, oxygen and MnO. Therefore, N_O and N_{MnO} represent the mole fractions of oxygen and MnO in the solid solution, respectively.

The oxides MnO and Mn_3O_4 were confirmed to be stable, whereas the higher oxides Mn_2O_3 and MnO_2 were not stable. This has also been reported by van Roosmalen et al. in the investigation of the pseudobinary La_2O_3-Mn_2O_3 phase diagram in the atmosphere of air (Fig. 6 in Ref. 18). They showed that below about 1150K, Mn_2O_3 is

stable, but at about 1150～1450K, t-Mn_3O_4 is stable.

3-1-2. Er_2O_3-MnO-MnO_2 system.

Four samples with Er_2O_3/MnO molar ratios of 0.5/0.5, 0.4/0.6, 0.25/0.75, and 0.15/0.85 were prepared for thermogravimetric analysis. The relationships between the oxygen partial pressure, (−log (P_{O_2}/atm)), on the ordinate and the ratio of weight changes, (W_{O_2}/W_T), on the abscissa are shown for three representative samples of 0.15/0.85, and 0.4/0.6 in Figs. 1- (a) and (b). Here, W_{O_2} is the weight increase of the samples from the reference weight at log (P_{O_2}/atm) = −12.00, at which Er_2O_3 and MnO are stable, and W_T is the total weight gain from the reference state to the weight at 1 atm O_2, at which Er_2O_3 and $ErMnO_3$ or $ErMnO_3$ and Mn_3O_4 are stable, depending on the total composition of the samples. As can be seen in the figures, the weight gradually changes with oxygen partial pressure due to the presence of solid solutions. Weight breaks are found at −log (P_{O_2}/atm) = 7.95 and 5.40. The value log (P_{O_2}/atm) = −5.40, corresponds to the value at which MnO and Mn_3O_4 are in equilibrium. Table 1 shows the results of phase identification in the Er-Mn-O system. Samples of around 500 mg were prepared for the identification of phases using the quenching method. Four phases, Er_2O_3, MnO, Mn_3O_4, and $ErMnO_3$ were found to be stable. $ErMn_2O_5$, $Er_2Mn_2O_7$, $ErMn_2O_4$, Mn_2O_3 and MnO_2 were not stable.

Based on the results of thermogravimetric analysis and phase identification, a phase diagram was constructed for the Er_2O_3-MnO-MnO_2 system, even though MnO_2 was not stable under these conditions, as shown in Fig. 2. The numerical values shown for three of the solid fields in Fig. 2 were the −log (P_{O_2}/atm) values at equilibrium,

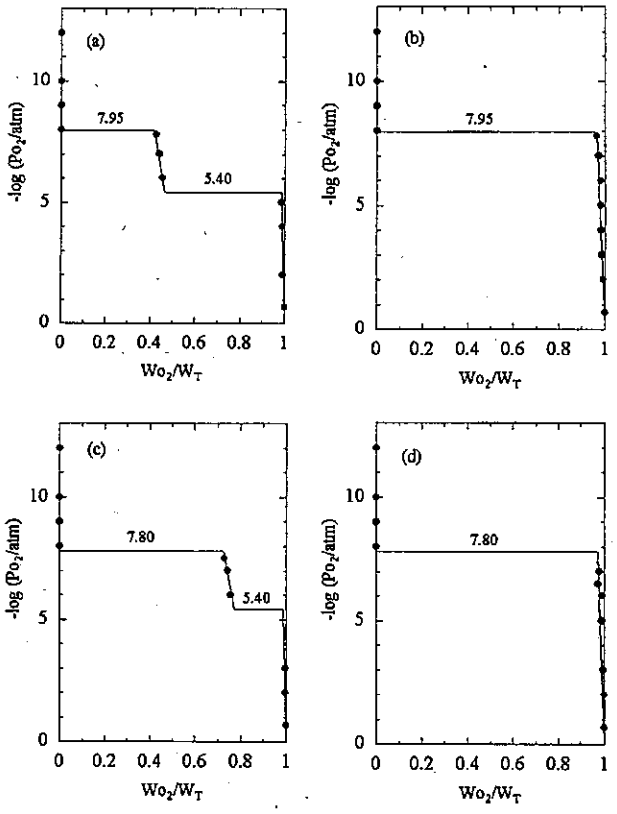

Fig. 1. The relationship between the oxygen partial pressure, log (P_{O_2}/atm), and the weight change of the samples, W_{O_2}/W_T. (a) Er_2O_3/MnO = 0.15/0.85, (b) Er_2O_3/MnO = 0.4/0.6, (c) Tm_2O_3/MnO = 0.25/0.75, and (d) Tm_2O_3/MnO = 0.50/0.50.

Table 1. Identification of Phases

Sample		−log (P_{O_2}/atm)	Time/h	Phase
Er_2O_3	MnO			
0.5	0.5	10.00	23	Er_2O_3 + MnO
		9.00	24	Er_2O_3 + MnO
		7.50	24	Er_2O_3 + $ErMnO_3$
		6.00	24	Er_2O_3 + $ErMnO_3$
		0.68	91	Er_2O_3 + $ErMnO_3$
0.25	0.75	10.00	23	Er_2O_3 + MnO
		9.00	24	Er_2O_3 + MnO
		7.50	24	$ErMnO_3$ + MnO
		6.00	24	$ErMnO_3$ + MnO
		5.00	24	$ErMnO_3$ + Mn_3O_4
		0.68	91	$ErMnO_3$ + Mn_3O_4
0.15	0.85	10.00	23	Er_2O_3 + MnO
		9.00	24	Er_2O_3 + MnO
		7.50	24	$ErMnO_3$ + MnO
		6.00	24	$ErMnO_3$ + MnO
		5.00	24	$ErMnO_3$ + Mn_3O_4
		0.68	91	$ErMnO_3$ + Mn_3O_4
Tm_2O_3	MnO			
0.50	0.50	11.00	7	Tm_2O_3 + MnO
		9.00	16	Tm_2O_3 + MnO
		7.50	23	Tm_2O_3 + $TmMnO_3$
		0.68	45	Tm_2O_3 + $TmMnO_3$
0.20	0.80	11.00	7	Tm_2O_3 + MnO
		9.00	16	Tm_2O_3 + MnO
		7.50	23	$TmMnO_3$ + MnO
		6.50	23	$TmMnO_3$ + MnO
		5.00	24	$TmMnO_3$ + Mn_3O_4
		0.68	45	$TmMnO_3$ + Mn_3O_4
0.10	0.90	1.00	7	Tm_2O_3 + MnO
		9.00	16	Tm_2O_3 + MnO
		7.50	23	$TmMnO_3$ + MnO
		6.50	23	$TmMnO_3$ + MnO

as indicated. As shown in Fig. 2, there are two three-phase regions, R + A_1 + D_1 and A_2 + P_2 + M, in which the oxygen partial pressures at equilibrium are 7.95 and 5.40 in −log (P_{O_2}/atm), respectively. It is important to note that there are five two-phase regions, Er_2O_3-MnO, Er_2O_3-$ErMnO_3$, MnO-$ErMnO_3$, MnO-Mn_3O_4, and Mn_3O_4-$ErMnO_3$. $ErMnO_3$ exhibits non-stoichiometric compositions in the range of log P_{O_2} = −7.95 (P_1) to 0 (P_3), as shown in Fig. 2. A perovskite-structured $LaMnO_{3+\delta}$ solid solution was reportedly to able to form with excess La as well as with excess Mn by van Roosmalen et al.(18). The same phenomenon does not appear in this three-component system. The relationship between the oxygen partial pressure and the ratio N_O/N_{ErMnO_3} is represented by the equation $N_O/N_{ErMnO_3} = 2.675 \times 10^{-3}$ (log P_{O_2}) − 0.008. Here, N_O and N_{ErMnO_3} show the mole fraction of oxygen and $ErMnO_3$ in the $ErMnO_3$ solid solution, respectively.

Table 2 lists the compositions, symbols, oxygen partial pressures in equilibrium, and activities of the components in solid solution applying the same symbols used in Fig. 2. The standard state of the solid solutions was arbitrarily set as log a_i = 0.

Lattice constants of the $ErMnO_3$ with the hexagonal system are listed in Table 3. A sample having Er_2O_3/MnO ratio of 0.25/0.75 was quenched in air. The phase coexisting with $ErMnO_3$ is indicated in the last column of Table 3. Present values show a small difference from previous values (19).

3-1-3. Tm_2O_3-MnO-MnO_2 system.

Six samples with Tm_2O_3/MnO molar ratios of 0.6/0.4, 0.5/0.5, 0.3/0.7, 0.25/0.75, 0.2/0.8 and 0.1/0.9 were prepared for thermogravimetric analysis. Fig.1 shows the relationships between the oxygen partial pressure, $-\log (P_{O_2}/atm)$, on the ordinate and the weight change, W_{O_2}/W_T, on the abscissa for two representative samples, 0.5/0.5 (Fig. 1(c)) and 0. 1/0.9 (Fig. 1(d)). Here, W_{O_2} is the weight increase of the samples from the reference weight at $\log(P_{O_2}/atm) = -12.00$, at which Tm_2O_3 and MnO are stable, and W_T is the total weight gain from the reference state to the weight at 1 atm O_2, at which both Tm_2O_3 and $TmMnO_3$, and $TmMnO_3$ and Mn_3O_4 are stable, depending on the total composition of the samples.

Table 2.Compositions, Symbols, Stability Ranges in Oxygen Partial Pressure, and Activities of Components in Solid Solutions.

Component	Compositions	Symbols	$-\log (P_{O_2}/atm)$	$\log a_i$
MnO	$MnO_{1.00}$	A	10.00~12.00	0
	$MnO_{1.00}$	A_1	7.95	-1.03×10^{-3}
	$MnO_{1.00}$	A_2	7.80	-1.00×10^{-3}
	$MnO_{1.02}$	A_3	5.40	-1.37×10^{-2}
$ErMnO_3$	$ErMnO_{2.97}$	P_1	7.95	0
	$ErMnO_{2.98}$	P_2	5.40	0.25
	$ErMnO_{3.00}$	P_3	0.00	0.074
$TmMnO_3$	$TmMnO_{2.98}$	P_4	7.55	0
	$TmMnO_{2.98}$	P_5	5.40	0.091
	$TmMnO_{3.00}$	P_6	0.00	0.054

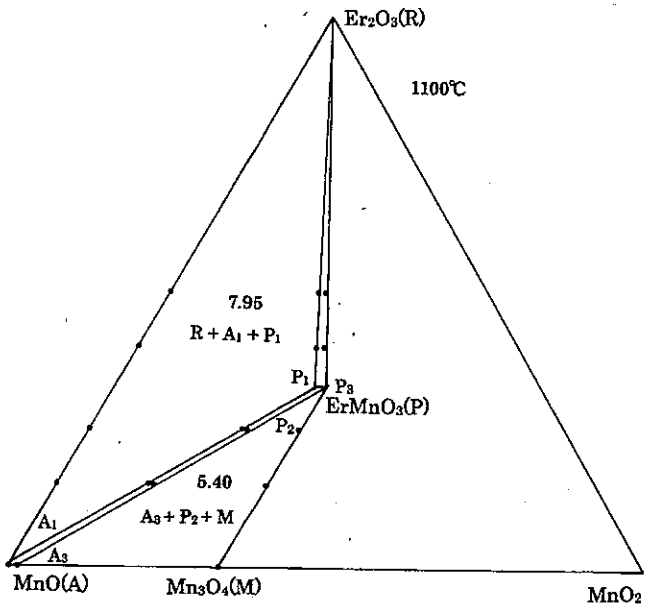

Fig. 2. Phase equilibrium in the Er_2O_3-MnO-MnO_2 system at 1100℃. Numerical values indicated in the three-solidphase regions are the oxygen partial pressure in $-\log (P_{O_2}/atm)$ in equilibrium with three solid phases which are shown in the regions. Abbreviations are the same as those in Table 2.

Weight breaks are found at $-\log (P_{O_2}/atm) = 7.80$ and 5.40. These values correspond to the oxygen partial pressure at which the three-solid phases, Tm_2O_3 (R) + $TmMnO_3$ (P_4) + MnO (A_2) and $TmMnO_3$ (P_5) + MnO (A_3) + Mn_3O_4 (M) are in equilibrium, respectively. The partial pressure $\log P_{O_2} = -5.40$ corresponds to the equilibrium between MnO and Mn_3O_4, as described above.

The results of phase identification of the Tm-Mn-O system are shown in Table 1,

along with those of the Er_2O_3-MnO-MnO_2 system. Four phases, Tm_2O_3, MnO, Mn_3O_4, and $TmMnO_3$, were found to be stable, whereas $TmMn_2O_5$, $Tm_2Mn_2O_7$, $TmMn_2O_4$, Mn_2O_3 and MnO_2 were not stable in the present experimental setup.

Table 3. Lattice constants of Quenched $ErMnO_3$ and $TmMnO_3$

Sample	$-\log P_{O_2}$ (atm)	a (A)	c (A)	V (A^3)	Coexisted Phase
Er_2O_3 MnO 0.25 0.75	0.68	6.126(4)	11.372(2)	369.6(6)	Mn_3O_4
Ref. 19		6.1166	11.435		
Tm_2O_3 MnO 0.2 0.8	0.68	6.082(4)	11.385(6)	364.8(3)	Mn_3O_4
Ref. 20		6.016	11.376		

Based on the above thermogravimetric results And phase identifications, a phase diagram was constructed for the Tm_2O_3-MnO-MnO_2 system, even though MnO_2 is not stable under the experimental conditions, and this is shown in Fig. 3. The numerical values shown in the three-phase regions of Fig. 3 are the $-\log (P_{O_2}/atm)$ values found for the three solid phases, as described above. Abbreviations are the same as those in Table 2. It is important to note that there are five two-phase regions. $TmMnO_3$ has a small non-stoichiometric composition in the range of $\log (P_{O_2}/atm) = -7.80$ to 0. Although it is a short range for a solid solution, the relation N_O/N_{TmMnO_3} vs. the oxygen partial pressure $\log (P_{O_2}/atm)$ for the $TmMnO_3$ solid solution was calculated from the present phase diagram. The following equation was obtained: $N_O/N_{TmMnO_3} = 2.530\times10^{-3} (\log P_{O_2}) - 0.005$.

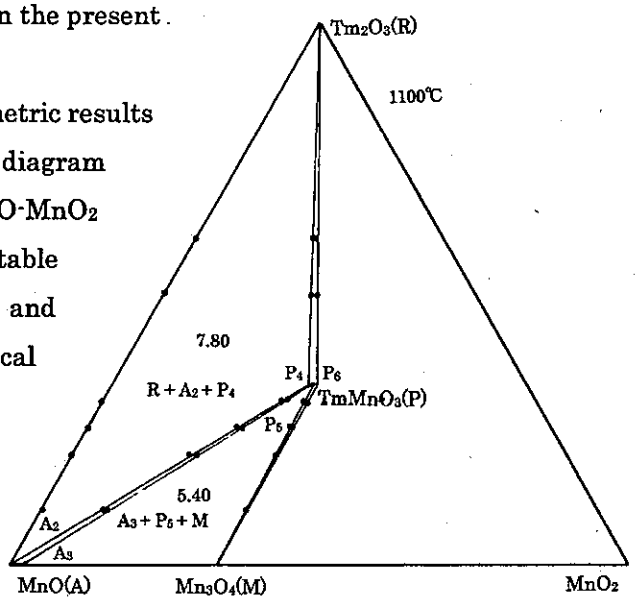

Fig. 3. Phase equilibrium in the Tm_2O_3-MnO-MnO_2 system at 1100℃. Numerical values indicated in the three-solid phase regions are the oxygen partial pressure in $-\log (P_{O_2}/atm)$ in equilibrium with three solid phases which are shown in the regions. Abbreviations are the same as those in Table 2.

The lattice constants of the hexagonal $TmMnO_3$ are listed in Table 3, together with the values of $ErMnO_3$. A sample with Tm_2O_3/MnO ratios of 0.2/0.8 was quenched in air, $-\log (P_{O_2}/atm) = 0.68$. Phases coexisting with $TmMnO_3$ are shown in the last column in Table 3. A large difference was found between our lattice constants of $TmMnO_3$ and previously cited values (20).

3-2. The Standard Gibbs Energy Change of a Reaction

Based on the established phase diagrams, the standard Gibbs energy changes of the reactions corresponding to the phase diagrams were determined from the equation, $\Delta G^\circ = -RT \ln K$, where R is the gas constant, T the absolute temperature, and K the equilibrium constant of the reaction. The results obtained are listed in Table 4. The standard state of the activities of the components in the solid solutions can be arbitrarily chosen for each solid solution as indicated by $\log a_i = 0$ in Table 2. The $-\log (P_{O_2}/atm)$ values and ΔG^0 columns shown in parentheses in Table 4 are calculated from quoted ΔG^0 and $\log (P_{O_2}/atm)$ values, respectively.

Table 4. The standard Gibbs Energy Changes of the Reaction at 1100℃.

Reaction	$-\log P_{O_2}$ (atm)	$-\Delta G^\circ$ (kJ/mol)
(1) $3MnO + 1/2\ O_2 = Mn_3O_4$	5.40	72.1
	5.40	75.0
	(5.62)	73.9[a]
	(4.60)	60.4[b]
	(3.87)	50.9[c]
(2) $1/2\ Er_2O_3 + MnO + 1/4\ O_2 = ErMnO_3$	7.95	52.3
	8.01[d]	(53.7)
(3) $1/2\ Tm_2O_3 + MnO + 1/4\ O_2 = TmMnO_3$	7.80	51.3
	7.90	51.9[d]

Ref. 21: [b] Ref. 22 : [c] Ref. 23: [d] Ref. 24:
The values in parentheses are calculated from the quoted ΔG^0 or the oxygen partial pressures.

The standard Gibbs energy change for reaction (1) is -72.1 ± 0.3 kJ/mol. Assuming that the MnO activity of the composition (A_3) is unified, -75.0 ± 0.3 kJ/mol is obtained, as shown in the second line of Table 4. This difference between the values is due to the small solid solution range. And this value is very similar to the results obtained by Hahn et al.(21). But their other two values are larger by about 10～20 $kJmol^{-1}$ than the present values. The results for reactions (2) and (3) are in good agreement with those obtained by Atsumi et al.(24), even though the experimental methods were different.

3-3. Relationship between tolerance factor and ΔG°

The reaction $1/2\ Ln_2O_3 + MnO + 1/4\ O_2 = LnMnO_3$, is common to all of the Ln-Mn-O systems studied so far. The relationship between the ΔG^0 values of this reaction and the tolerance factor (t) of perovskite structures with 12-coordinated lanthanoid atoms is shown in Fig. 4. Previously reported values (7, 8, 9, 10, 11, 12) of ΔG^0 are also shown in Fig. 4 for comparison. The solid circles represent values for orthorhombic system, and open circles represent values for hexagonal systems. Ionic radii given by Espinosa (25) were used to calculate the tolerance factors. The ionic

radii for Er and Tm are 1.276 A and 1.271 A from 12-coordinated garnet, respectively, and the ionic radius of O^{2-} was taken to be 1.40 A. The crystal structurs of $ErMnO_3$ and $TmMnO_3$ are hexagonal. Thus, it may be problematic to adapt tolerance factors based upon the orthorhombic perovskite structure to both hexagonal oxides. As can be seen in Fig. 4, the Gibbs energy change of the reacton was nearly proportional to the tolerance factor for a perovskite structure. The values of Er and Tm are well fitted to the equation, ΔG^0 (hexa) = -5.885×10^2 t + 4.908×10^2 that was presented by Kitayama et al.(12). This is shown by a dotted line, and ΔG^0 (ortho) vs. tolerance factor (t) is shown by a solid line in Fig. 4.

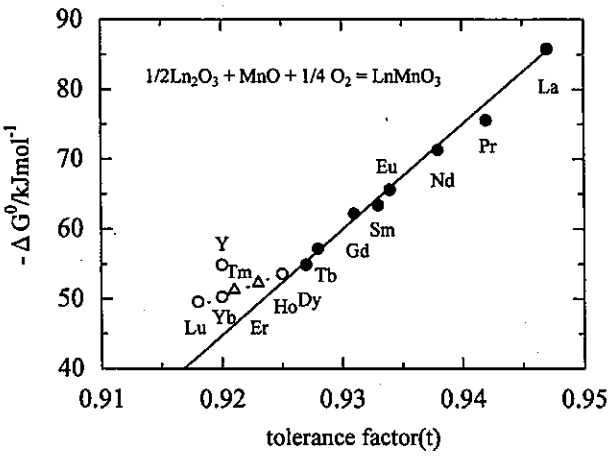

Fig. 4

Fig. 4. The relationship between the ΔG^0 value of the reaction, 1/2 Ln_2O_3 + MnO + 1/4 O_2 = $LnMnO_3$, and the tolerance factor (t). Solid circles indicate previous values for orthorhombic systems, and open circles represent previous values for hexagonal systems. The open triangles are the present values of $ErMnO_3$ and $TmMnO_3$. These values are well-fitted to the hexagonal line.

3-4. The Gibbs energy change of the phase transition

So far, in the series of the Ln-Mn-O system, the reaction, 1/2 Ln_2O_3 + MnO + 1/4 O_2 = $LnMnO_3$, has been found to be common. We have obtained two such reactions, namely:

① 1/2 Ln_2O_3 + MnO + 1/4 O_2 = $LnMnO_3$ (ortho) ΔG^0 (ortho)

② 1/2 Ln_2O_3 + MnO + 1/4 O_2 = $LnMnO_3$ (hexa) ΔG^0 (hexa)

Here, $LnMnO_3$ (ortho) and $LnMnO_3$ (hexa) and ΔG^0 (ortho) and ΔG^0 (hexa) denote the manganite of orthorhombic and hexagonal crystal $LnMnO_3$ and the Gibbs energy changes of reactions ① and ②, respectively.

Deducting equation ② from ①, we find equation ③:

③ $LnMnO_3$ (hexa) = $LnMnO_3$ (ortho) $\Delta G^0(3) = \Delta G^0$ (ortho) $- \Delta G^0$ (hexa)

This equation shows the transition from the hexagonal to the orthorhombic system. Here, $\Delta G^0(3)$ is the Gibbs energy change of reaction (3), that is, the Gibbs energy change of the transition from the hexagonal to the orthorhombic system.

Assuming that the ΔG^0 (ortho) of $ErMnO_3$ and $TmMnO_3$ can be extrapolated by the equation, ΔG^0 (ortho) = -1.518×10^3 t + 1.352×10^3 (from La to Tb), we can obtain ΔG^0(3) for the above manganites by calculation. The results are tabulated in Table 5.

Table 5 Estimated ΔG^0 (trans)/kJmol^{-1} values for $ErMnO_3$ and $TmMnO_3$

$LnMnO_3$	t	$-\Delta G^0$ (hexa)	$-\Delta G^0$ (ortho)*	ΔG^0 (trans)
$ErMnO_3$	0.923	52.3	49.1	3.2
$TmMnO_3$	0.921	51.3	46.1	5.2

* Extrapolated values calculated from the general equation for orthorhombic $LnMnO_3$.

The ΔG^0 (trans) values for $ErMnO_3$ and $TmMnO_3$ are 3.2 and 5.2 kJmol-1, respectively. So, these reactions do not take place in the hexagonal to orthorhombic direction at 1100℃. This means that physical energy (for example $P\Delta V$) is needed in order for the reaction ③ to take place from left to right. That is, if a volume change (ΔV) were to be found, from the hexagonal system to the orthorhombic system of $ErMnO_3$ and $TmMnO_3$, the pressure (P) could be estimated and ascertained by a high pressure apparatus.

4. Conclusion

1) Phase equilibria in the system Ln-Mn-O (Ln = Er and Tm) at 1100℃ were established under an oxygen partial pressure ranging from 0 to −12.00 in log(P_{O_2}/atm).

2) Under the present experimental conditions, the Ln_2O_3, MnO, Mn_3O_4, and $LnMnO_3$ phases are stable in both systems.

3) MnO, $ErMnO_3$, and $TmMnO_3$ have non-stoichiometric composition. However, Mn_3O_4 is stoichiometric. The ranges of non-stoichiometry for both $ErMnO_3$ and $TmMnO_3$ are very small.

4) The lattice constants of quenched $ErMnO_3$, and of $TmMnO_3$ were determined and compared with previous values. The values we obtained are not in agreement with the previous values.

5) The standard Gibbs energies of the reactions found in the diagram were calculated with the oxygen partial pressure in equlibrium with three solid phases.

6) ΔG^0 values for the reaction, 1/2 Ln_2O_3 + MnO + 1/4 O_2 = $LnMnO_3$, for hexagaonal $ErMnO_3$ and $TmMnO_3$, fit the linear equation of the tolerance factor (t) vs. ΔG^0

ΔG^0 (hexa) = -6.426×10^2 t + 5.406×10^2.

7) The Gibbs energy changes of the transition, $ErMnO_3$ (hexa) = $ErMnO_3$ (ortho) and

$TmMnO_3$ (hexa) and $TmMnO_3$ (ortho), were determined as 3.2 and 5.2 $kJmol^{-1}$, under assumption that the ΔG^0 (ortho) value equation for $ErMnO_3$ and $TmMnO_3$ was applicable .

References

1) J. B. Goodenough, Phys. Rev., 103, 564 (1955).

2) C. N. R. Rao, Annu. Rev. Phys. Chem., 40, 291(1989).

3) B. C. Hauback, H. Fjellvag, and N. Sakai, J. Solid State Chem., 124, 43 (1996).

4) J. A. M. Van Roosmalen and E. H. P. Cordfunke, J. Solid State Chem., 93, 212 (1991), J. A. M. Roosmalen, E. H. P. Cordfunke, and R. B. Helmholdt, 110, 100 (1994), J. A. M. Roosmalen and E. H. P. Cordfunke, 110, 106 (1994), 110, 109 (1994), 110, 113 (1994).

5) V. A. Cherepanov, L. Yu. Barkhatova, A. N. Petrov, and V. I Voronin, J. Solid State Chem., 118, 53 (1995).

6) N. Kamegashira and Y. Miyazaki, Mat. Res. Bull., 19, 1201 (1984).

7) K. Kitayama, J. Solid State Chem., 153, 336 (2000).

8) K. Kitayama and T. Kanzaki, J. Solid State Chem., 158, 236 (2001).

9) K. Kitayama, H. Ohno, R. Ide, K. Satoh, and S. Murakami, J. Solid State Chem., 166, 285 (2002).

10) K. Kitayama, M. Kobayashi, and T. Kimoto, J. Solid State Chem., 167, 160 (2002).

11) K. Kitayama, H. Ohno, M. Kurahashi, E. Koizumi, and M. Inagaki, J. Solid State Chem., 174, 249 (2003).

12) K. Kitayama, M. Kobayashi, H. Takano, N. Nambu, and H. Hirasawa, J. Solid State Chem.,176, 151 (2003).

13) K. Kitayama, T. Yazaki, T. Fukushima, K. Matsui, S. Sami, and M. Nakamura, Res. J. Chem. Environ., 9 (2), 55 (2005).

14) K. Kitayama and T. Yazaki, Res. J. Chem. Environ., 9(4), 27 (2005).

15) K. Kitayama, K. Nojiri, T. Sugihara, and T. Katsura, J. Solid State Chem., 56, 1 (1985).

16) K. Kitayama, J. Solid State Chem., 137, 255 (1998).

17) T. Katsura and H. Hasegawa, Bull. Chem. Soc. Jpn., 40, 561 (1967).

18) J. A. M. van Roosmalen, P. van Vlaanderen, E. H.P. Cordfunke, W. L. Ijdo, and D. J. W. Ijdo, J. Solid State Chem., 114, 516 (1995).

19) JCPDS Card 14-0689

20) JCPDS Card 25-1075

21) W. C. Jr. Hahn and A. Muan, Am. J. Sci., 258, 66 (1960).

22) R. A. Robie et al. "Thermodynamic Properties of Minerals and Related Substances at 298.15 K and 1 Bar (10^5 Pascals) Pressure and at Higher Temperatures", Geological Survey Bulletin 1452 , 1978.

23) J. F. Elliott and M. Gleiser, Thermochemistry for steelmaking, Vol. 1, Addison-Wesley, 1960.

24) T. Atsumi, T. Ohgushi, and N. Kamegashira, J. Alloys Compd. 234, 35 (1996)

25) G. P. Espinosa, J. Chem. Phys., 37, 2344 (1962).